

Initial Results on a New Light-Duty 2.7-L Opposed-Piston Gasoline Compression Ignition Multi-Cylinder Engine

Ashwin Salvi

Achates Power, Inc.,
San Diego, CA 92101
e-mail: salvi@achatespower.com

Reed Hanson

Achates Power, Inc.,
San Diego, CA 92121
e-mail: rmhanson2@wisc.edu

Rodrigo Zermeno

Achates Power, Inc.,
San Diego, CA 92121
e-mail: rodrigo.zermeno@ricardo.com

Gerhard Regner

Achates Power, Inc.,
San Diego, CA 92121
e-mail: regnertvc@achatespower.com

Mark Sellnau

Delphi Technologies,
Auburn Hills, MI 48326
e-mail: mark.sellnau@aramcoservices.com

Fabien Redon

Achates Power, Inc.,
San Diego, CA 92121
e-mail: redon@achatespower.com

Gasoline compression ignition (GCI) is a cost-effective approach to achieving diesel-like efficiencies with low emissions. The fundamental architecture of the two-stroke Achates Power Opposed-Piston (OP) Engine enables GCI by decoupling piston motion from cylinder scavenging, allowing for flexible and independent control of cylinder residual fraction and temperature leading to improved low-load combustion. In addition, the high peak cylinder pressure and noise challenges at high-load operation are mitigated by the lower brake mean effective pressure (BMEP) operation and faster heat release for the same pressure rise rate of the OP Engine. These advantages further solidify the performance benefits of the OP Engine and demonstrate the near-term feasibility of advanced combustion technologies, enabled by the opposed-piston architecture. This paper presents initial results from steady-state testing on a brand new 2.7-L OP GCI multi-cylinder engine (MCE) designed for light-duty truck applications. Successful GCI operation calls for a high compression ratio (CR), leading to higher combustion stability at low loads, higher efficiencies, and lower cycle HC + NO_x emissions. Initial results show a cycle average brake thermal efficiency (BTE) of 31.7%, which is already greater than 11% conventional engines, after only ten weeks of testing. Emissions results suggest that Tier 3 Bin 160 levels can be achieved using a traditional diesel after-treatment system. Combustion noise was well controlled at or below the United States Council for Automotive Research limits. In addition, initial results on catalyst light-off mode with GCI are also presented.

[DOI: 10.1115/1.4053518]

Keywords: air emissions from fossil fuel combustion, energy conversion/systems, fuel combustion, power (co-) generation, transportation

Opposed-Piston Engine Fundamentals

Reduced Heat Transfer Losses. The Achates Power Opposed-Piston Engine configuration has two pistons facing each other in the same cylinder, combining the stroke of both pistons to increase the effective stroke-to-bore ratio. The Opposed-Piston (OP) Engine architecture eliminates the cylinder head of a conventional engine, thus reducing the surface area-to-volume ratio, reducing heat transfer losses, and increasing thermal efficiency [1–6]. A conceptual comparison between a conventional engine and the OP Engine is shown in Fig. 1. At the same piston bore and stroke, the surface area-to-volume ratio is reduced by more than 30% for the OP Engine.

Further heat loss reductions are enabled due to higher wall temperatures of the two piston crowns from two-stroke operation compared to a cooling stroke and presence of a cylinder head in conventional engines, reducing the temperature differential between hot combustion gases and the wall.

An additional benefit of the reduced heat losses in the OP Engine is the reduction in radiator size and fan power, enabling lower vehicle drag losses and increasing vehicle fuel efficiency.

Lower Pumping Losses. The pistons in an OP Engine are decoupled from inducting fresh air and exhausting combustion products. The scavenging of the cylinder is governed by the pressure ratio across the intake and exhaust ports. Intake manifold pressure, air flowrate, and exhaust gas recirculation (EGR) rate are controlled by the supercharger, supercharger bypass valve, EGR valve, variable

geometry (VG) turbocharger, and backpressure valve positions (schematically shown in Fig. 2). This configuration minimizes engine pumping losses as the cylinder does not need to be fully scavenged every cycle, i.e., during idle or low-load conditions, only a fraction of the exhaust gases are scavenged and replaced with fresh air, just sufficient enough for the next combustion cycle. This architectural advantage is a key enabler to the flat fuel map of the OP Engine. Partial scavenging of the cylinder also enables control over the trapped residual fraction, enabling high combustion stability and rapid engine warm-up from cold start [7–9].

An additional pumping advantage of the OP Engine is the larger intake and exhaust port flow area compared to a conventional engine, reducing choked and restricted flow and further decreasing pumping losses.

Earlier and Faster Combustion. Equation (1) describes the first law of thermodynamics for conventional and OP Engines, where Q is the heat released, θ is the crank angle, γ is the ratio of specific heats, p is the cylinder pressure, and V is the cylinder volume. The larger combustion volume resulting from Fig. 1, highlighted by the grey boxes in Eq. (1), for the given amount of energy released also enables a shorter combustion duration while preserving the same maximum pressure rise rate [10]. The faster combustion improves thermal efficiency by reaching a condition closer to constant volume combustion.

Earlier combustion, closer to top dead center or minimum volume, provides higher indicated efficiency, but if combustion is too early, it can lead to increased heat transfer losses and lower efficiency. Combustion that is too far delayed in relation to minimum volume leads to higher exhaust energy and lower efficiency. The impact of heat transfer can be seen in Fig. 3. The lower surface area-to-volume ratio results in lower heat transfer losses in

Contributed by the Internal Combustion Engine Division of ASME for publication in the JOURNAL OF ENERGY RESOURCES TECHNOLOGY. Manuscript received October 1, 2021; final manuscript received January 5, 2022; published online February 9, 2022. Assoc. Editor: Cosmin E. Dumitrescu.

Engine	Conventional	OP Engine
Cylinders	6	3
Trapped Volume/Cylinder	1.0L	1.6L
Stroke/Bore Ratio	1.1	2.2
Trapped Compression Ratio	15:1	15:1
Combustion Chamber Surface Area/Volume (mm ⁻¹)	0.28	0.18

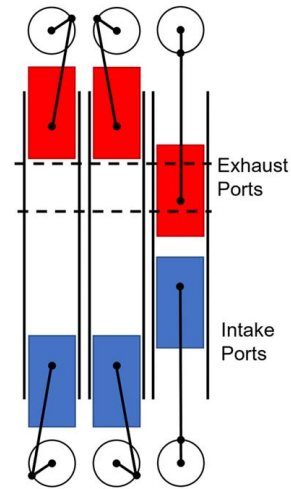


Fig. 1 OP Engine schematic, figure not to scale

the OP Engine, enabling combustion timing closer to minimum volume. This increases the effective expansion ratio and reduces fuel consumption compared to conventional engines.

Equation 1: First law of thermodynamics showing a faster rate of heat release with OP Engine at same pressure rise rate

1st Law of Thermodynamics:

Conventional Engine

$$\frac{dQ_{AS-AHR}}{d\theta} = \frac{\gamma}{\gamma-1} p \frac{dV}{d\theta} + \frac{1}{\gamma-1} V \frac{dp}{d\theta} \leftarrow \text{SAME}$$

OP Engine

$$\frac{dQ_{2S-AHR}}{d\theta} = \frac{\gamma}{\gamma-1} p \frac{d(1.6V)}{d\theta} + \frac{1}{\gamma-1} (1.6V) \frac{dp}{d\theta}$$

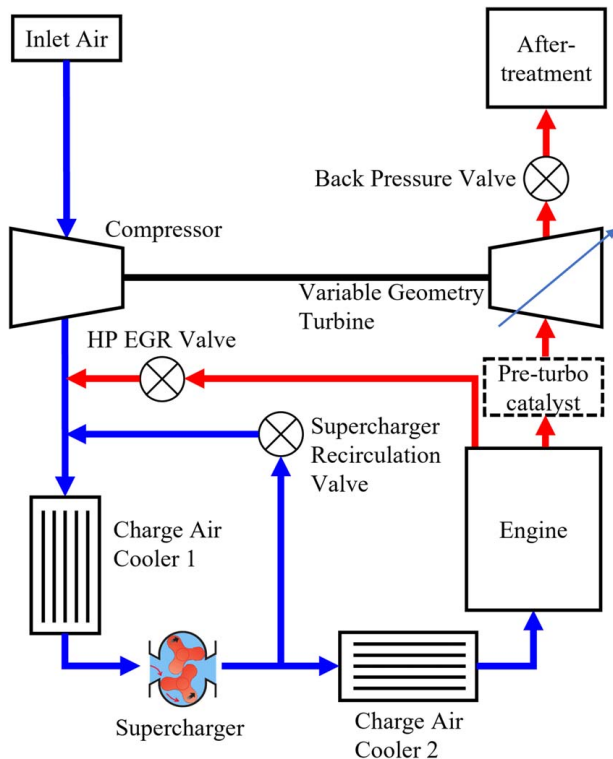


Fig. 2 OP Engine air handling schematic

Cleaner Combustion. Due to the elimination of the cylinder head, fuel is introduced tangentially to the piston surface; thus, the OP Engine does not use the piston to break apart the fuel spray as in conventional diesel engines. This allows for the optimization of the piston shape to generate high turbulent kinetic energy while minimizing combustion surface area-to-volume ratio therefore heat transfer, leading to improved spray atomization, vaporization, and lower soot emissions. An illustrative schematic of an OP combustion bowl and fuel injection event is shown in Fig. 4, highlighting the diametrically opposed injectors injecting fuel tangentially to the piston and the unique combustion volume. Additionally, the lower load two-stroke operation of the OP Engine and ability to retain internal EGR without incurring additional pumping work results in lower NO_x emissions.

Combining Opposed-Piston and Gasoline Compression Ignition

A significant amount of pioneering research has been conducted on gasoline compression ignition [11–25]. Traditional challenges with GCI arise at low-load conditions due to low charge

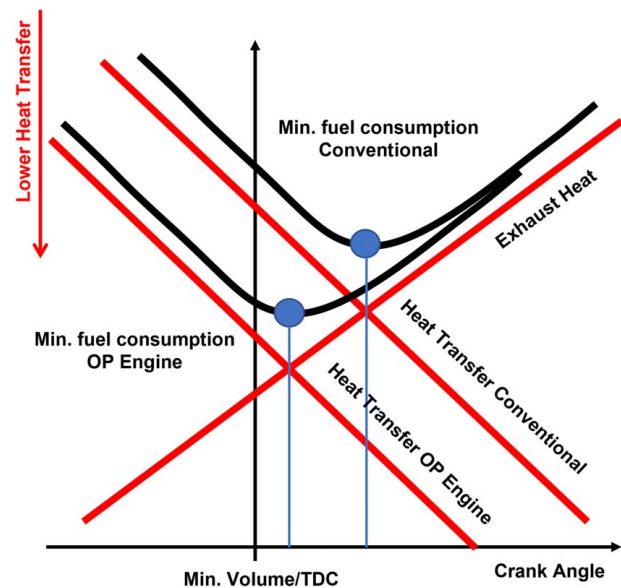


Fig. 3 Lower OP Engine heat transfer losses enable earlier combustion phasing for lower fuel consumption

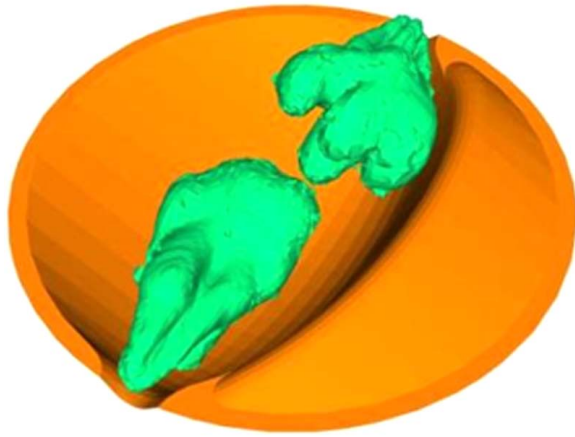


Fig. 4 Diametrically opposed fuel injectors injecting fuel tangentially to the piston surface

temperatures causing combustion instability and at high-load conditions due to peak cylinder pressure and noise limitations. The opportunities and lessons learned form the basis for GCI on the OP Engine, with the added benefit of the opposed-piston architecture addressing some of the four-stroke GCI challenges. The fundamental architecture of the OP Engine enables GCI by decoupling piston motion from cylinder scavenging, allowing for flexible and independent control of cylinder residual fraction and temperature leading to improved low-load combustion. In addition, the high peak cylinder pressure and noise challenges at high-load operation are mitigated by the lower brake mean effective pressure operation and faster heat release for the same pressure rise rate of the OP Engine.

Mixture Preparation. Robust and clean GCI combustion requires a stratified charge, with locally lean and rich areas, and multiple injection events. The OP injection environment offers significant potential to improve charge stratification. Diametrically opposed dual injectors spray across the diameter of the cylinder. Each injector can be independently controlled to more easily manage staggered injections for ideal mixture distribution and, therefore, efficient and controlled heat release [26,27].

Table 1 2.7-L OP GCI engine specifications

Displacement (L)	2.7
Cylinders	3
Compression ratio	18.5
(-)	
Power (kW)	200 @ 3600 RPM
Torque (Nm)	650 @ 1600–2100 RPM
Bore (mm)	80
Stroke (mm)	177
Exhaust crank lead (deg) ^a	8–12
Air handling	VG turbocharger, supercharger, high-pressure EGR
Fuel injection system	Delphi Technologies injectors, 2 per cylinder, capable of 6 injection events per injector
Engine control unit	Pi Innovo Open

^aExhaust crank lead defines an advancement of the exhaust piston in crank angle relation to the intake piston. This provides an exhaust blow-down event, promotes cylinder scavenging, and increases exhaust crankshaft torque.

Charge Temperature Management. At low loads, GCI requires higher temperatures for combustion than diesel fuel. Four-stroke engines normally push nearly the entire content of the cylinder out during the exhaust stroke and therefore require a complex variable valvetrain to re-open the exhaust valve during the intake stroke to re-induct the exhaust back in the cylinder to increase the charge temperature to the level necessary for GCI ignition.

The OP Engine, however, can retain exhaust gas in-cylinder after combustion, even at low loads when relatively little additional intake oxygen is required, by reducing the scavenging of the cylinder. At low loads, the OP Engine can reduce the supercharger work used to boost the intake manifold pressure. Reducing scavenging has four benefits: (1) it reduces the amount of work by the supercharger, reducing pumping; (2) it keeps in-cylinder temperatures high for good combustion stability; (3) it provides a natural or internal EGR effect for low NO_x combustion; and (4) it provides high exhaust gas temperatures for catalyst light-off and sustained activity.

2.7-L Opposed-Piston Multi-Cylinder Design

Engine Specifications. A new multi-cylinder OP Engine was designed and built from scratch and is geared toward the light-duty

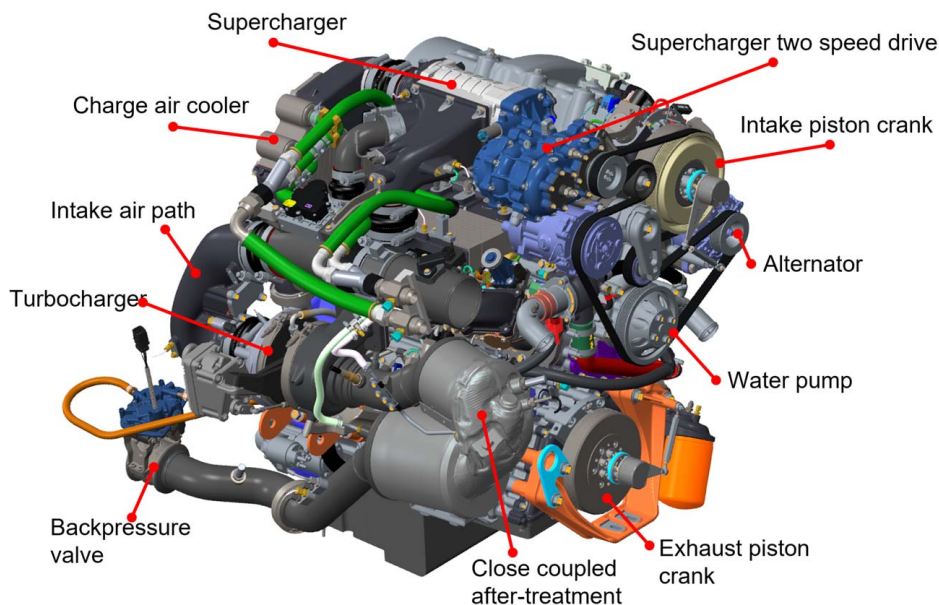


Fig. 5 Isometric computer-aided design (CAD) view of the new 2.7-L OP GCI engine

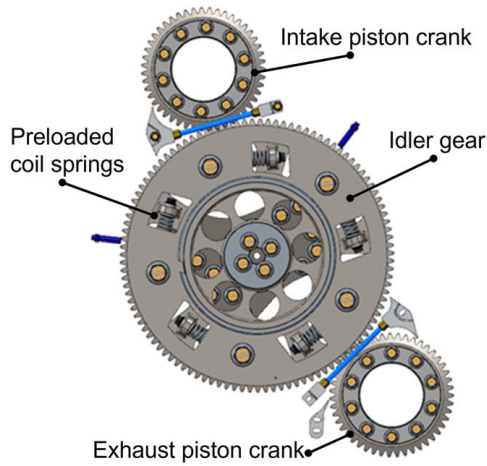


Fig. 6 2.7-L OP Engine geartrain connecting intake and exhaust crankshafts

vehicle sector. Specifications for the engine are shown in Table 1, with a labeled CAD image of the engine shown in Fig. 5.

The intake piston crank is located on top of the engine, with the exhaust piston crank on the bottom of the engine. The cylinders are tilted 30 deg from vertical to package into currently existing vehicles. The mechanical connection that links the two crankshafts together is a novel three gear geartrain, with power take-off on the exhaust crankshaft and is shown in Fig. 6.

The air handling of the engine is packaged on the opposite side of the tilted cylinders, giving the visual impression of a Vee-style engine. The airpath is as follows (Fig. 2): air is inducted by the turbocharger compressor, mixed with high-pressure EGR (HP EGR), cooled by a charge air cooler, compressed by a supercharger, flow is split between supercharger recirculation and flow through an intercooler, and finally into the intake chest. After combustion, exhaust gases split between the high-pressure EGR loop and VG turbine flow. After the VG turbocharger, the exhaust gas flows through a close-coupled after-treatment system (not studied in this paper), through a backpressure valve, through an underfloor selective catalyst reduction (SCR) (not studied in this paper), and then to the test cell air management system.

An electric water pump was used for engine cooling, and the power consumption is accounted for in the brake numbers presented. An alternator efficiency of 60% was assumed.

Fuel System Specifications. The fuel injection process and fuel sprays are key to achieving a successful combustion system with high efficiency, low emissions, and low combustion noise. The injection pressure requirement of 1800 bar is higher than gasoline fuel systems currently. Therefore, a diesel fuel system was specified for operation on US E10 gasoline with a lubricity additive.

A CAD rendering of the fuel system is shown in Fig. 7. It is comprised of two independent systems, each with one pump, one rail, high-pressure lines, and three injectors for each side of the engine. Two injectors are mounted diametrically opposed in each cylinder. The two fuel rails may be operated at different pressures. This configuration provides great flexibility in the injection process for fuel quantity, timing, and splits.

Two diesel unit pumps with roller lifters are mounted on the front cover of the engine and are driven simultaneously by the intake crankshaft with a three-lobe cam. The pumps (Fig. 8) are compact, are lubricated by engine oil, and are mechanically efficient.

The injectors shown in Fig. 7 were specially built for an opposed-piston engine operating on gasoline fuel. The injector features top feed fuel inlet, electrical connection on the body side, and short overall injector length (137 mm). Since gasoline fuels have very

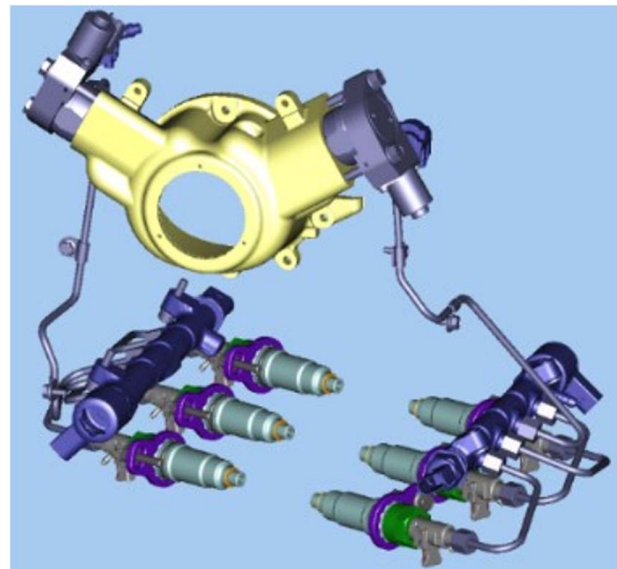


Fig. 7 2.7-L OP Engine fuel injection system, with two independent pumps, rails, and injectors

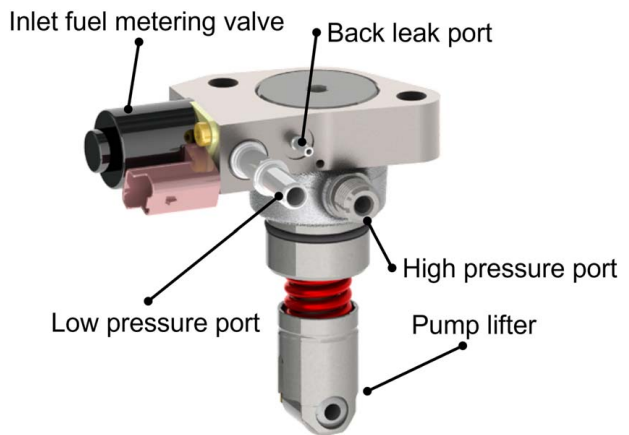


Fig. 8 Delphi Technologies diesel unit pump with roller lifter and inlet metering valve

low viscosity relative to diesel, back leak flows will be significantly increased, and more pump work will be required. This injector features a pressure balanced control valve, which greatly reduces back leak flows, especially at higher pressures. The injector features fast response for near square injection profiles. Figure 9 shows typical injection rate and drive current at 1200 bar fuel pressure.

Testing Specifications. Gasoline fuel specifications are shown in Table 2. The fuel flow is measured using a Resol fuel system (model number RS474BCX-40), the air flow is measured using a Meriam laminar flow element (model number Z50MH10-5), CO, O₂, CO₂, and HC emissions are measured using a California Analytical Instruments (CAI) emissions analyzer, NO_x emissions are measured using a MKS Fourier-transform infrared (FTIR) spectrometer, and soot values are measured with an AVL 415 smoke meter.

Initial Results

Initial Cycle Average Results. The following results are after only ten weeks of testing the brand new 2.7-L OP GCI engine. Operating the engine over a 10-mode steady-state representation of the

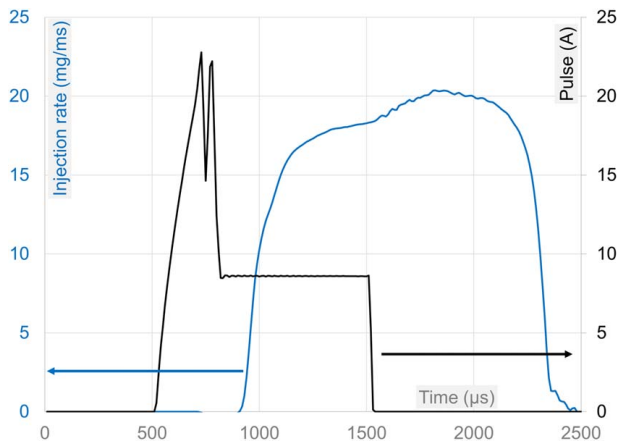


Fig. 9 Injection rate and drive current at 1200-bar fuel pressure

Table 2 Gasoline fuel specifications

Fuel	Gasoline
Ethanol (%vol)	10
Research octane number (-)	91
Motor octane number (-)	83
Antiknock Index (-)	87

Table 3 2.7L OP GCI hot LA4 cycle average results

BSFC	272.1	g/kWh	BSNO _x	2.0	g/kWh
ISFC	204.7	g/kWh	BSSoot	0.03	g/kWh
BTE	31.7	% Fuel	BSCO	3.5	g/kWh
ITE	42.1	% Fuel	BSHC	1.3	g/kWh
Pumping loss	1.8	% Fuel	FTP75 NO _x	0.82	g/mi
Friction loss	8.5	% Fuel	FTP75 Soot	0.011	g/mi
			FTP75 HC	0.553	g/mi

transient Federal Test Procedure 75 (FTP75) cycle yields a cycle average BTE of 31.7% on the hot LA4 cycle (Table 3, modal data provided in the next section). Even after minimal development time, the engine is already showing an 11% BTE improvement compared to a competitive Model Year (MY) 2015 four-stroke engine.¹

Table 3 also shows the cycle average emissions. The initial targets for the OP GCI engine are U.S. Environmental Protection Agency (EPA) light-duty (LD) Tier 3 Bin 160, which has a tailpipe NMOG + NO_x requirement of 160 mg/mile, CO requirement of 4.2 g/mile, and PM requirement of 3 mg/mile, and a final target of U.S. EPA light-duty Tier 3 Bin 30. An initial modeling study with an after-treatment supplier using off-the-shelf diesel after-treatment components and the 10-mode approximation of a transient cycle indicated the successful achievement of Bin 160 levels. Tier 3 Bin 30 emissions levels are expected with a gasoline-specific after-treatment implementation of catalyst thermal management, and an actual transient cycle instead of a steady-state approximation.

A sample cylinder pressure, combustion profile, and fuel injection traces are shown in Fig. 10 at 1275 RPM, 173 Nm of torque. An early pilot is utilized during the compression stroke of the engine and a main injection event near the minimum volume location, which is similar to other published works [13,15,28]. The early timing is required to overcome the longer ignition delay of gasoline fuel and

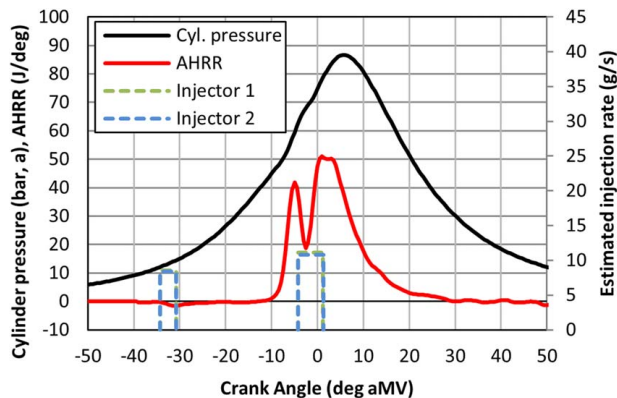


Fig. 10 Cylinder pressure, combustion profile, and fuel injection traces at 1275 RPM, 173 Nm

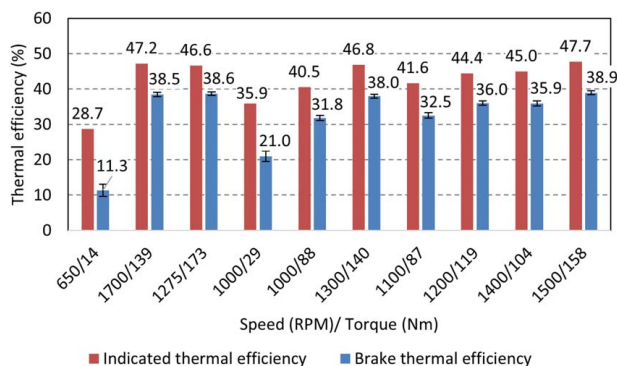


Fig. 11 GCI indicated and brake thermal efficiency over 10 modes

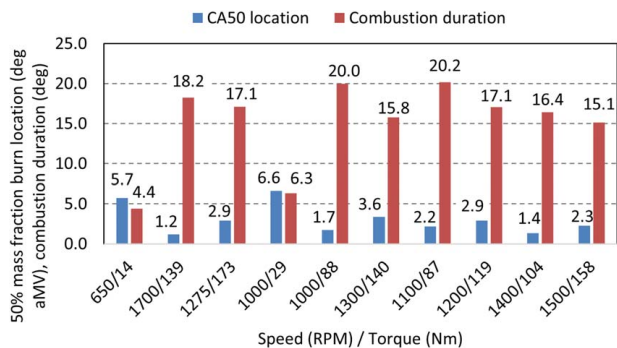


Fig. 12 50% mass fraction burn location and combustion duration

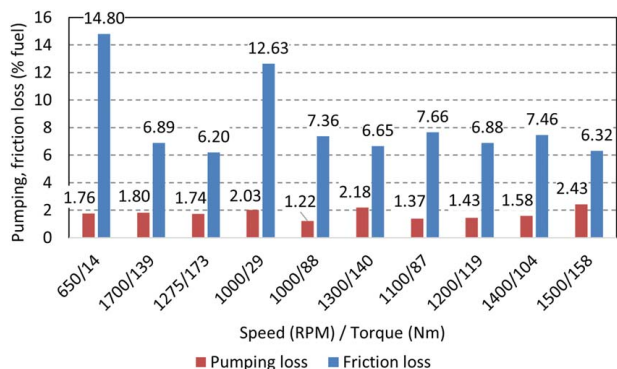


Fig. 13 Pumping and friction loss over 10 modes

¹<https://www.epa.gov/vehicle-and-fuel-emissions-testing/benchmarking-advanced-low-emission-light-duty-vehicle-technology-test-data>, 2018. Accessed June 1, 2018.

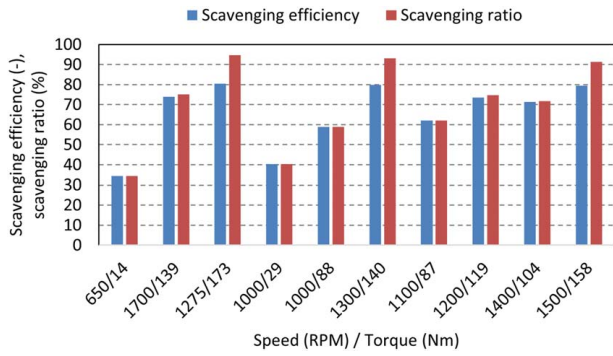


Fig. 14 Scavenging efficiency and scavenging ratio over the 10 modal points

helps to premix part of the fuel with air, creating a homogenized mixture. The main injection timing occurs around the premixed combustion spike of the pilot fuel mixture. This serves to control the rate of heat release, reducing combustion noise and increasing combustion controllability. The main injection event results in a diffusion flame, similar to that of diesel combustion. The fuel split between the pilot and the main at this condition is 30% pilot, 70% main; however, the split depends on the engine load.

Modal Data. Figure 11 shows the preliminary indicated and brake thermal efficiencies across the 10 modes. This preliminary

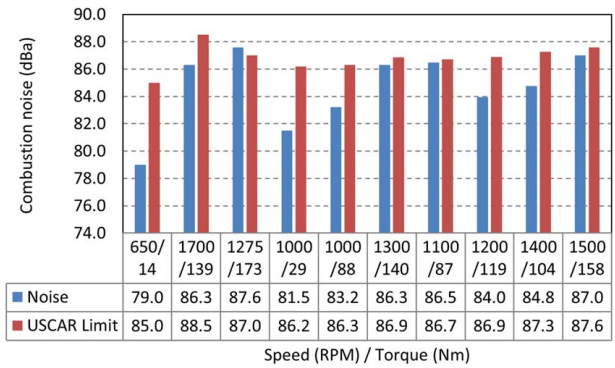


Fig. 16 GCI measured combustion noise and USCAR noise limits

data illustrates the high thermal efficiencies of the OP GCI engine at part load/low-load conditions, which is due to lower heat transfer losses and lower pumping work inherent to the opposed-piston architecture. Figure 12 illustrates the 50% mass fraction burn location for the 10 modes, in degrees after minimum volume (aMV). As stated earlier in Fig. 3, the 50% mass fraction burn location tends to be earlier, and combustion duration tends to be shorter for the OP Engine.

The pumping loss resulting from supercharger work (Fig. 13), while lower for the OP Engine compared to conventional engines, has considerable opportunity for improvement through cylinder ports, turbocharger, and backpressure optimization. As this paper

LA4 Cycle Averaged Friction Breakdown

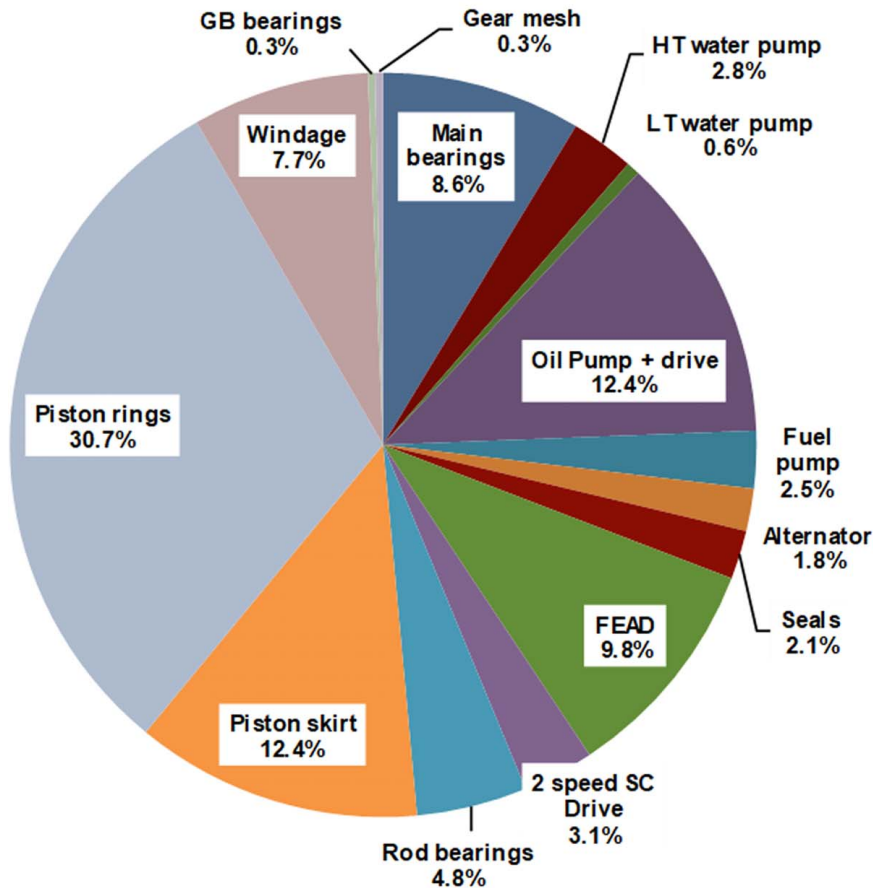


Fig. 15 2.7-L OP Engine friction breakdown

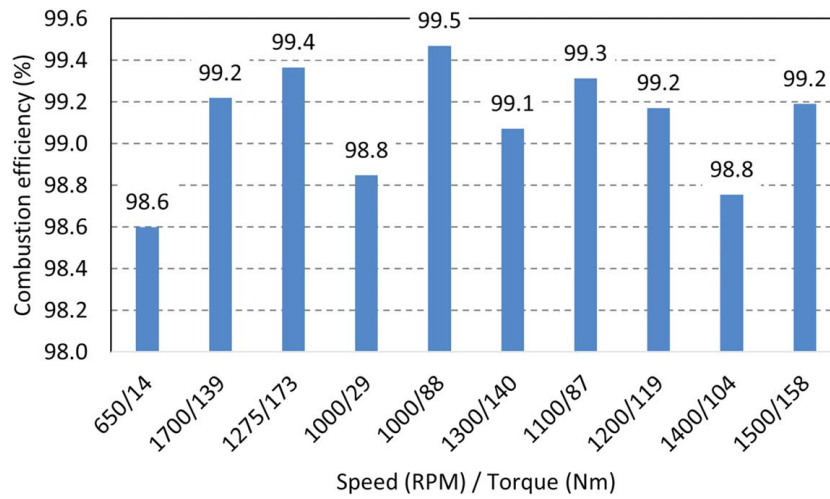


Fig. 17 GCI combustion efficiency over 10 modes

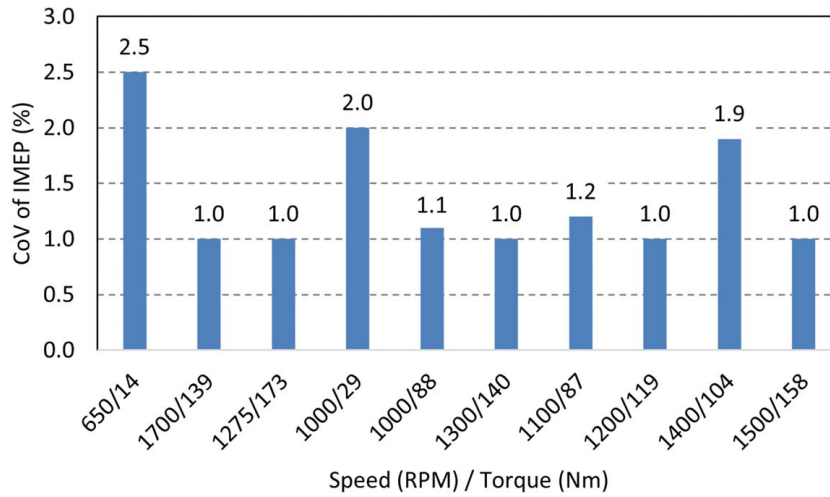


Fig. 18 GCI CoV of IMEP over 10 modes

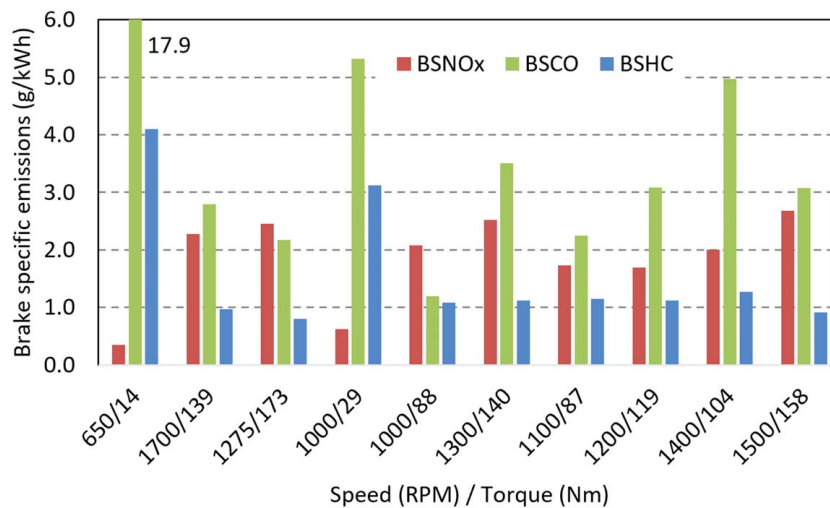


Fig. 19 Brake-specific NO_x, CO, HC over 10 modes

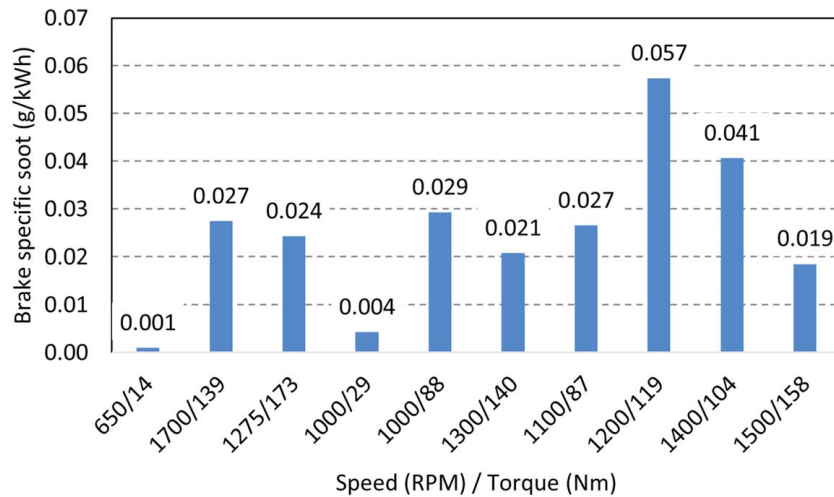


Fig. 20 Brake-specific soot over 10 modes

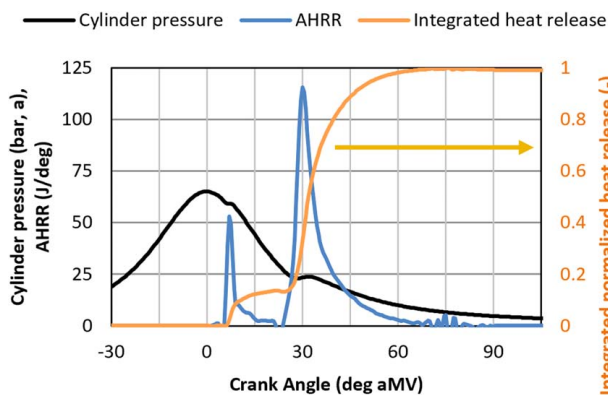


Fig. 21 Catalyst light-off mode with gasoline compression ignition

discusses initial results from the new engine, air path optimization is the subject of future work. The friction loss increases at low loads due to the low fueling quantity and low engine out power. However, friction reduction is expected for production-intent designs as this prototype incorporated off the shelf components that were not optimized for use on this engine.

Pumping is required to scavenge the cylinder and introduce a fresh charge for the next combustion cycle. Two scavenging metrics related to pumping loss are scavenging efficiency (ratio of delivered air mass retained to mass of trapped cylinder charge) and scavenging ratio (ratio of delivered air mass to mass of trapped cylinder charge) and are shown in Fig. 14. For most cases, the scavenging efficiency is similar to the scavenging ratio. However, when the scavenging ratio is greater than scavenging efficiency, the fresh charge is escaping the cylinder through the exhaust ports, incurring additional pumping loss. As load increases, the scavenging ratio starts to exceed scavenging efficiency due to the boost and airflow required to meet efficiency and emissions targets for that speed and load point.

The friction loss from the engine is also shown in Fig. 13. The new 2.7-L engine incorporated several frictional improvements over the research-grade Achates Power 4.9-L multi-cylinder engine discussed in previous publications [8,29]; however, additional friction improvements are still in development. The current friction breakdown for an LA4 cycle averaged speed and load point is illustrated in Fig. 15. Piston rings are identified as the higher contributor to OP Engine friction, followed by the piston skirt and oil pump, and are active areas of research.

Combustion noise was well controlled at or below the guidelines from United States Council for Automotive Research (USCAR) ² at all of the points except one, as shown in Fig. 16. The ability of the OP Engine to control scavenging, the high flexibility of the fuel injection system, and the high-pressure fuel injection strategy are all key enablers in controlling the pressure rise rate and combustion noise. The high compression ratio (CR) enabled by GCI operation enables more favorable autoignition characteristics from increased cylinder pressure and temperature, stretching out combustion slightly compared to lower compression ratio configurations, further reducing combustion noise. Combustion noise is a calibration parameter and can be adjusted to meet relevant requirements.

The higher compression ratio enabled by GCI operation also achieves high combustion efficiency, yielding gasoline combustion efficiencies that are greater than 98.5% at all points (Fig. 17). The combustion efficiencies are very similar to diesel values, however are generated with gasoline fuel. The ability to reduce cylinder scavenging at low loads, which lowers the pumping work of the engine, also enables high trapped temperatures. The hotter cylinder charge enables better fuel vaporization and higher chemical kinetic rates, leading to more robust, low coefficient of variation (CoV) of indicated mean effective pressure (IMEP) combustion (Fig. 18).

The brake-specific oxides of nitrogen (BSNO_x), brake-specific carbon monoxide (BSCO), and brake-specific hydrocarbons (BSHC) values are shown in Fig. 19, with BSNO_x as a calibration target. Higher compression ratios tend to increase NO_x emissions; however, the combination of lower BMEP operation of the OP Engine combined with lower temperature combustion with gasoline compression ignition compared to diesel keep NO_x formation low. BSCO and BSHC values are low, especially compared to an early injection strategy with GCI [10], due in part to the higher compression ratio of the engine as well as the higher combustion efficiency [30]. Even though higher compression ratios increase NO_x from the higher cylinder temperatures, the decreased HC and CO emissions lower the overall non-methane organic gas (NMOG) + NO_x total emission.

The resulting brake-specific soot (BSSoot) is shown in Fig. 20. The partial pre-mixing of the fuel with an early pilot homogenizes the cylinder charge and lower soot formation. The main injection event then controls the rate of heat release and lowers combustion noise as shown previously. The high volatility and partial oxygenation of gasoline fuel promote better fuel mixing and availability of oxygen, further reducing soot formation, especially during diffusion combustion.

²<https://uscar.org/publications/>, 2018. Accessed June 1, 2018.

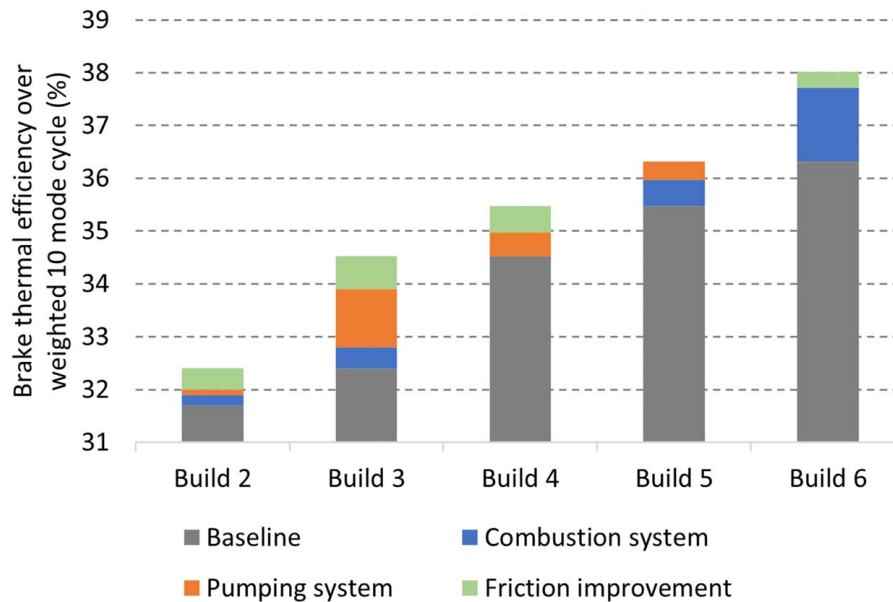


Fig. 22 Anticipated cycle brake thermal efficiency improvements with respect to program targets

Catalyst Light-Off Mode. Previous papers [8,9] have discussed the unique ability of the OP Engine for rapid after-treatment catalyst light-off and emissions control using diesel fuel. To understand the commercial and emissions potential of GCI, catalyst light-off mode was explored in a separate 1.6-L single-cylinder version of the opposed-piston engine.

Figure 21 highlights the cylinder pressure, rate of heat release, and integrated normalized heat release representative of an elevated idle condition using gasoline fuel. A similar injection strategy (pilot and main) is used in this condition and, however, is phased much later in the expansion stroke.

The flexibility of the scavenging and combustion system in the OP Engine allows for trapping high-temperature residuals, which enables robust and stable gasoline combustion ignition with a 1.1% CoV of IMEP, even with a combustion phasing of 30 deg after minimum volume. Catalyst light-off mode generates high IMEP with low BMEP and results in 365 °C exhaust gas temperature while keeping emissions low at 1 g/kWh NO_x and 0.01 g/kWh soot. The hot exhaust gases combined with low emissions during cold start are essential to satisfying stringent emissions requirements.

Conclusions

A brand new 2.7-L multi-cylinder OP Engine was designed and built to integrate into a light-duty pickup truck. The cylinders are tilted 30 deg from vertical, balanced by the air system on the opposite side and giving the engine the appearance of a Vee shape. The engine uses a high-pressure fuel system capable of generating different rail pressures for the two common rails for combustion flexibility. Engine friction results are encouraging, with piston rings contributing the most; however, frictional improvements are an active research area.

Initial results show a cycle average brake thermal efficiency of 31.7%, which is already greater than 11% conventional engines, after only ten weeks of testing. Combustion noise was well controlled at or below the USCAR limits. For a given NO_x calibration, soot emissions were very low. The cleaner combustion of gasoline fuel enabled the use of a higher compression ratio, which increased engine thermal efficiency while reducing low-load CoV of IMEP and combustion noise. The increased compression ratio increased combustion efficiency, reducing HC and CO emissions.

Catalyst light-off mode was explored with GCI. The flexibility of the OP Engine architecture to control scavenging and the controllability of the fuel injection system created stable combustion while generating hot exhaust gas at very low emissions. The combination of hot exhaust gases and low emissions lights off the emissions system quickly, satisfying stringent emissions requirements and enabling transition to high-efficiency strategies more quickly. After-treatment simulations using initial results and off-the-shelf diesel components show successful achievement of Tier 3 Bin 160 levels, with an end target of Tier 3 Bin 30.

Future Work

After only 10 weeks of development, the new 2.7-L OP GCI engine is already significantly more efficient than comparable gasoline engines. Considerable efforts are in progress to increase the brake thermal efficiency from the current 31.7% cycle average to 36.5% with advancements in friction, pumping, and combustion. Friction reduction tasks include reducing piston and liner friction, geartrain windage, and coolant and oil circuits. Tasks related to reducing pumping loss include optimizing scavenging, increasing air handling efficiency, and reducing system restriction. Combustion improvements stem from optimization of the combustion chamber, optimization of fuel injection parameters, and reducing heat transfer losses from the combustion volume. The details of the increase in brake thermal efficiency are proprietary; however, a schedule of the anticipated improvements is shown in Fig. 22 along with the program target.

Acknowledgment

The authors would like to thank the U.S. Department of Energy's Advanced Research Projects Agency—Energy (ARPA-E) for their intellectual and financial support. The information, data, or work presented herein was funded in part by the ARPA-E, U.S. Department of Energy, under Award Number DE-AR0000657. The views and opinions of authors expressed herein do not necessarily state or reflect those of the United States Government or any agency thereof. The authors would also like to specifically acknowledge the contribution of their colleagues in this work, namely Argonne National Laboratory, Delphi Technologies, and ARPA-E.

Conflict of Interest

There are no conflicts of interest.

Data Availability Statement

The data and information that support the findings of this article are freely available at: www.achatespower.com.

Nomenclature

- AHRR = apparent heat release rate
- BSFC = brake-specific fuel consumption
- CA50 = crank angle location of 50% mass fraction burned
- ISFC = indicated-specific fuel consumption
- ITE = indicated thermal efficiency
- LP EGR = low pressure EGR
- NO_x = nitrogen oxides
- SCE = single-cylinder engine
- SOI = start of injection

References

- [1] Herold, R. E., Wahl, M. H., Regner, G., Lemke, J. U., and Foster, D. E., 2011, "Thermodynamic Benefits of Opposed-Piston Two-Stroke Engines," SAE Paper No. 2011-01-2216.
- [2] Redon, F., Kalebjian, C., Kessler, J., Rakovec, N., Headley, J., Regner, G., and Koszewnik, J., 2014, Meeting Stringent 2025 Emissions and Fuel Efficiency Regulations With an Opposed-Piston, Light-Duty Diesel Engine," Paper No. SAE 2014-01-1187.
- [3] Regner, G., Johnson, D., Koszewnik, J., Dion, E., Redon, F., and Fromm, L., 2013, "Modernizing the Opposed Piston, Two Stroke Engine for Clean, Efficient Transportation," SAE Paper No. 2013-26-0114.
- [4] Warey, A., Gopalakrishnan, V., Potter, M., Mattarelli, E., and Rinaldini, C. A., 2016, "An Analytical Assessment of the CO2 Emissions Benefit of Two-Stroke Diesel Engines," SAE Paper No. 2016-01-0659.
- [5] Mattarelli, E., Rinaldini, C. A., Savioli, T., Warey, A., Gopalakrishnan, V., and Potter, M., 2018, "An Innovative Hybrid Powertrain for Small and Medium Boats," SAE Paper No. 2018-01-0373.
- [6] Mattarelli, E., Cantore, G., Rinaldini, C. A., and Savioli, T., 2017, "Combustion System Development of an Opposed Piston 2-Stroke Diesel Engine," *Energy Procedia*, **126**, pp. 1003–1010.
- [7] Kalebjian, C., Redon, F., and Wahl, M. H., 2012, "Low Emissions and Rapid Catalyst Light-Off Capability for Upcoming Emissions Regulations With an Opposed-Piston, Two-Stroke Diesel Engine," Proceedings of the Emissions 2012 Conference, Ypsilanti, MI, June 12–13, Volume 68.
- [8] Redon, F., Sharma, A., and Headley, J., 2015, "Multi-Cylinder Opposed Piston Transient and Exhaust Temperature Management Test Results," SAE Paper No. 2015-01-1251.
- [9] Patil, S., Ghazi, A., Redon, F., Sharp, C., Schum, D., and Headley, J., 2018, "Cold Start HD FTP Test Results on Multi-Cylinder Opposed-Piston Engine Demonstrating Rapid Exhaust Enthalpy Rise to Achieve Ultra Low NO_x," SAE Paper No. 2018-01-1378.
- [10] Regner, G., Koszewnik, J., and Venugopal, R., 2014, "Optimizing Combustion in an Opposed-Piston, Two-Stroke (OP2S) Diesel Engine," Internationaler Motorenkongress 2014: Antriebstechnik im Fahrzeug, J. Liebl, ed., Springer Vieweg, Wiesbaden, pp. 657–659.
- [11] Hanson, R., Splitter, D., and Reitz, R. D., 2009, "Operating a Heavy-Duty Direct-Injection Compression-Ignition Engine With Gasoline for Low Emissions," SAE Paper No. 2009-01-1442.
- [12] Sellnau, M., Sinnamon, J., Hoyer, K., and Husted, H., 2011, "Gasoline Direct Injection Compression Ignition (GDCI)—Diesel-Like Efficiency With Low CO₂ Emissions," *SAE Int. J. Engines*, **4**(1), pp. 2010–2022.
- [13] Sellnau, M., Hoyer, K., Moore, W., Foster, M., Sinnamon, J., and Klemm, W., 2018, "Advancement of GDCI Engine Technology for US 2025 CAFE and Tier 3 Emissions," SAE Paper No. 2018-01-0901.
- [14] Kalghatgi, G., Risberg, P., and Ångström, H.-E., 2007, "Partially Pre-Mixed Auto-Ignition of Gasoline to Attain Low Smoke and Low NO_x at High Load in a Compression Ignition Engine and Comparison With a Diesel Fuel," SAE Paper No. 2007-01-23.
- [15] Ra, Y., Loeper, P., Andrie, M., Krieger, R., Foster, D. E., Reitz, R. D., and Durrett, R., 2012, "Gasoline DICI Engine Operation in the LTC Regime Using Triple-Pulse Injection," *SAE Int. J. Eng.*, **5**(3), pp. 1109–1132.
- [16] Manente, V., Zander, C.-G., Johansson, B., Tunestal, P., and Cannella, W., 2010, "An Advanced Internal Combustion Engine Concept for Low Emissions and High Efficiency from Idle to Max Load Using Gasoline Partially Premixed Combustion," SAE Paper No. 2010-01-2198.
- [17] Subramanian, S. N., and Ciatti, S., 2011, "Low Cetane Fuels in Compression Ignition Engine to Achieve LTC," Proceedings of the ASME 2011 Internal Combustion Engine Division Fall Technical Conference, Morgantown, WV, Oct. 2–5, pp. 317–326.
- [18] Dec, J. E., Yang, Y., Dermotte, J., and Ji, C., 2015, "Effects of Gasoline Reactivity and Ethanol Content on Boosted, Premixed and Partially Stratified Low-Temperature Gasoline Combustion (LTGC)," *SAE Int. J. Engines*, **8**(3), pp. 935–955.
- [19] Benajes, J., Martin, J., Novella, R., and De Lima, D., 2014, "Analysis of the Load Effect on the Partially Premixed Combustion Concept in a 2-Stroke HSDI Diesel Engine Fueled With Conventional Gasoline," SAE Paper No. 2014-01-1291.
- [20] Rose, K. D., Ariztegui, J., Cracknell, R. F., Dubois, T., Hamje, H. D. C., Pellegrini, L., Rickeard, D. J., Heuser, B., Schnorbus, T., and Kolbeck, A. F., 2013, "Exploring a Gasoline Compression Ignition (GCI) Engine Concept," SAE Paper No. 2013-01-0911.
- [21] Paz, J., Staaden, D., and Kokjohn, S., 2018, "Gasoline Compression Ignition Operation of a Heavy-Duty Engine at High Load," SAE Paper No. 2018-01-0898.
- [22] Kavuri, C., and Kokjohn, S. L., 2018, "Computational Study to Identify Feasible Operating Space for a Mixed Mode Combustion Strategy—A Pathway for Premixed Compression Ignition High Load Operation," *ASME J. Energy Resour. Technol.*, **140**(8), p. 082201.
- [23] Dempsey, A., Curran, S., Wagner, R., and Cannella, W., 2015, "Effect of Premixed Fuel Preparation for Partially Premixed Combustion With a Low Octane Gasoline on a Light-Duty Multi-Cylinder Compression Ignition Engine," *ASME J. Eng. Gas Turbines Power*, **137**(11), p. 111506.
- [24] Zhang, Y., Voice, A., Pei, Y., Traver, M., and Cleary, D., 2018, "A Computational Investigation of Fuel Chemical and Physical Properties Effects on Gasoline Compression Ignition in a Heavy-Duty Diesel Engine," *ASME J. Energy Resour. Technol.*, **140**(10), p. 102202.
- [25] Kavuri, C., Singh, S., Rajan Krishnan, S., Kumar Srinivasan, K., and Ciatti, S., 2014, "Computational Analysis of Combustion of High and Low Cetane Fuels in a Compression Ignition Engine," *ASME J. Eng. Gas Turbines Power*, **136**(12), p. 121506.
- [26] Redon, F., 2016, "Exploring the Next Frontier in Efficiency With the Opposed-Piston Engine," SIA Powertrain, Rouen, France. R-2016-01-29.
- [27] Hanson, R., Strauss, S., Redon, F., and Salvi, A., 2017, "Progress in Light-Duty OPGCI Engine Design and Testing," SIA Powertrain, Versailles, France.
- [28] Kolodziej, C. P., Sellnau, M., Cho, K., and Cleary, D., 2016, "Operation of a Gasoline Direct Injection Compression Ignition Engine on Naphtha and E10 Gasoline Fuels," *SAE Int. J. Engines*, **9**(2), pp. 979–1001.
- [29] Sharma, A., and Redon, F., 2016, "Multi-Cylinder Opposed-Piston Engine Results on Transient Test Cycle," SAE Paper No. 2016-01-1019.
- [30] Hanson, R., Salvi, A., Redon, F., and Regner, G., 2018, "Experimental Comparison of GCI and Diesel Combustion in a Medium-Duty Opposed-Piston Engine," Proceedings of the ASME ICEF 2018 Internal Combustion Engine Division Fall Technical Conference Volume 1: Large Bore Engines; Fuels; Advanced Combustion, San Diego, CA, Nov. 4–7, ASME, p. V001T03A023.